

# Fisher Task Distance and Its Applications in Transfer Learning and Neural Architecture Search

Cat P. Le, Mohammadreza Soltani, Juncheng Dong, Vahid Tarokh

Duke University

Durham, North Carolina, USA

{cat.le, mohammadreza.soltani, juncheng.dong, vahid.tarokh}@duke.edu

## Abstract

We formulate an asymmetric (or non-commutative) distance between tasks based on Fisher Information Matrices. We provide proof of consistency for our distance through theorems and experiments on various classification tasks. We then apply our proposed measure of task distance in transfer learning on visual tasks in the Taskonomy dataset. Additionally, we show how the proposed distance between a target task and a set of baseline tasks can be used to reduce the neural architecture search space for the target task. The complexity reduction in search space for task-specific architectures is achieved by building on the optimized architectures for similar tasks instead of doing a full search without using this side information. Experimental results demonstrate the efficacy of the proposed approach and its improvements over other methods.

## Introduction

This paper is motivated by a common assumption made in transfer and lifelong learning: similar tasks usually have similar neural architectures. Building on this intuition, we propose a non-commutative measure, called *Fisher Task Distance* (FTD), which represents the complexity of transferring the knowledge of one task to another. FTD is defined in terms of the Fisher Information matrix defined as the second-derivative of the loss function with respect to the parameters of the models under consideration. By definition, FTD is always greater or equal to 0, where the equality holds if and only if it is the distance from a task to itself. To show that our task distance is mathematically well-defined, we provide some theoretical analysis. Moreover, we empirically verify that the FTD is statistically a consistent distance through experiments on numerous tasks and datasets. Next, we instantiate our proposed task distance on two important AI applications, Transfer Learning (TL) and Neural Architecture Search (NAS). In particular, we demonstrate how the FTD identifies the related tasks and utilizes the gained knowledge for transfer learning. The experiments on the visual tasks in Taskonomy (Zamir et al. 2018) dataset indicate our computational efficiency while achieving similar results as the brute-force approach proposed by Zamir et al. (2018). Next, we apply the proposed task distance in the NAS framework, learning an appropriate architecture for

a target task based on its similarity to other learned tasks. For a target task, the closest task in a given set of baseline tasks is identified and its corresponding architecture is used to construct a neural search space for the target task without requiring prior domain knowledge. Subsequently, a gradient-based search algorithm called FUSE (Le et al. 2021) is applied to discover an appropriate architecture for the target task. Briefly, the utilization of the related tasks' architectures helps reduce the dependency on prior domain knowledge, consequently reducing the search time for the final architecture and improving the robustness of the search algorithm. Extensive experimental results for the classification tasks on MNIST (LeCun, Cortes, and Burges 2010), CIFAR-10, CIFAR-100 (Krizhevsky, Hinton et al. 2009), and ImageNet (Russakovsky et al. 2015) datasets demonstrate the efficacy and superiority of our proposed approach compared to the state-of-the-art approaches.

## Related Works

The task similarity has been mainly considered in the transfer learning (TL) literature. Similar tasks are expected to have similar architectures as manifested by the success of applying transfer learning in many applications (Silver and Bennett 2008; Finn et al. 2016; Mihalkova, Huynh, and Mooney 2007; Niculescu-Mizil and Caruana 2007; Luo et al. 2017; Razavian et al. 2014; Pan and Yang 2010). However, the main goal in TL is to transfer trained weights from a related task to a target task. Recently, a measure of closeness of tasks based on the Fisher Information matrix has been used as a regularization technique in transfer learning (Chen, Zhang, and Dong 2018) and continual learning (Kirkpatrick et al. 2017) to prevent catastrophic forgetting. Additionally, the task similarity has also been investigated between visual tasks in (Zamir et al. 2018; Pal and Balasubramanian 2019; Dwivedi and Roig. 2019; Achille et al. 2019; Wang, Wehbe, and Tarr 2019; Standley et al. 2020). These works only focus on weight-transfer and do not utilize task similarities for discovering the high-performing architectures. Moreover, the introduced measures of similarity from these works are often assumed to be symmetric which is not typically a realistic assumption. For instance, consider learning a binary classification between cat and dog images in the CIFAR-10 dataset. It is

easier to learn this binary task from a pre-trained model on the entire CIFAR-10 images with 10 classes than vice versa.

In the context of the neural architecture search (NAS), the similarity between tasks has not been explicitly considered. Most NAS methods focus on reducing the complexity of search by using an explicit architecture search domain and specific properties of the given task at hand. NAS techniques have been shown to offer competitive or even better performance to those of hand-crafted architectures. In general, these techniques include approaches based on evolutionary algorithms (Real et al. 2019; Sun et al. 2021), reinforcement learning (Zoph and Le 2017), and optimization-based approaches (Liu et al. 2018). However, most of these NAS methods are computationally intense and require thousands of GPU-days operations. To overcome the computational issues and to accelerate the search procedure, recently, differentiable search methods (Cai, Zhu, and Han 2019; Liu, Simonyan, and Yang 2018; Noy et al. 2019; Luo et al. 2018; Xie et al. 2018; Wan et al. 2020; Awad, Mallik, and Hutter 2020; He et al. 2020) have been proposed. These methods, together with random search methods (Li et al. 2018; Li and Talwalkar 2020; Sciuto et al. 2019) and sampling sub-networks from one-shot super-networks (Zoph et al. 2018; Bender et al. 2018; Li and Talwalkar 2020; Cho, Soltani, and Hegde 2019; Yang et al. 2020), can significantly speed up the search time in the neural architecture space. Additionally, some reinforcement learning methods with weight-sharing (Pham et al. 2018; Song et al. 2021; Bender et al. 2020), similarity architecture search (Le et al. 2021; Nguyen et al. 2020), neural tangent kernel (Chen, Gong, and Wang 2021), network transformations (Cai et al. 2018; Elsken, Metzen, and Hutter 2019; Jin, Song, and Hu 2018; Hu et al. 2019), and few-shot approaches (Cai et al. 2019; Zhou et al. 2020; Zhang et al. 2020; Zhao et al. 2020) have yielded time-efficient NAS methods. None of these approaches consider the task similarities in their search space. In contrast, our approach exploits asymmetric relation between tasks to reduce the search space and accelerate the search procedure.

## Fisher Task Distance

Before discussing the task distance, we recall the definition of the Fisher Information matrix for a neural network.

**Definition 1** (Fisher Information Matrix). *Let  $N$  be a neural network with data  $X$ , weights  $\theta$ , and the negative log-likelihood loss function  $L(\theta) := L(\theta, X)$ . The Fisher Information Matrix is defined as follows:*

$$F(\theta) = \mathbb{E} \left[ \nabla_{\theta} L(\theta) \nabla_{\theta} L(\theta)^T \right] = -\mathbb{E} \left[ \mathbf{H}(L(\theta)) \right], \quad (1)$$

where  $\mathbf{H}$  is the Hessian matrix, i.e.,  $\mathbf{H}(L(\theta)) = \nabla_{\theta}^2 L(\theta)$ , and expectation is taken w.r.t the distribution of data.

In practice, we use the empirical Fisher Information Matrix computed as follows:

$$\hat{F}(\theta) = \frac{1}{|X|} \sum_{i \in X} \nabla_{\theta} L^i(\theta) \nabla_{\theta} L^i(\theta)^T, \quad (2)$$

---

### Algorithm 1: Fisher Task Distance

---

**Data:**  $X_a = \{X_a^{(1)} \cup X_a^{(2)}\}$ ,  $X_b = \{X_b^{(1)} \cup X_b^{(2)}\}$

**Input:**  $\varepsilon$ -approx. network  $N$

**Output:** Distance from task  $a$  to task  $b$

```

1 Function TaskDistance ( $X_a^{(1)}, X_b, N$ ):
2   Initialize  $N_a, N_b$  from  $N$ 
3   Train  $N_a$  using  $X_a^{(1)}$ ,  $N_b$  using  $X_b^{(1)}$ 
4   Compute  $F_{a,b}$  (equation 2) using  $X_b^{(2)}$  on  $N_a$ 
5   Compute  $F_{b,b}$  (equation 2) using  $X_b^{(2)}$  on  $N_b$ 
6   return  $d[a, b] = \frac{1}{\sqrt{2}} \left\| F_{a,b}^{1/2} - F_{b,b}^{1/2} \right\|_F$ 

```

---

where  $L^i(\theta)$  is the loss value for the  $i^{\text{th}}$  data in the set  $X$ <sup>1</sup>.

Consider a dataset  $X = X^{(1)} \cup X^{(2)}$  with  $X^{(1)}$  and  $X^{(2)}$  denote the training and the test data, respectively. Let's denote a task  $T$  and its corresponding dataset  $X$  jointly by a pair  $(T, X)$ . Also, let  $\mathcal{P}_N((T, X^{(2)})) \in [0, 1]$  be a function that measures the performance of a given architecture  $N$  on a task  $T$  using the test dataset  $X^{(2)}$ .

**Definition 2** ( $\varepsilon$ -approximation Network for Task  $T$ ). *An architecture  $N$  is called an  $\varepsilon$ -approximation network for task  $T$  and the corresponding data  $X$  if it is trained using training data  $X^{(1)}$  such that  $\mathcal{P}_N(T, X^{(2)}) \geq 1 - \varepsilon$ , for a given  $0 < \varepsilon < 1$ .*

In practice, architectures for  $\varepsilon$ -approximation networks for a given task  $T$  are selected from a pool of well-known hand-designed architectures.

**Definition 3** (Fisher Task Distance). *Let  $a$  and  $b$  be two tasks with  $N_a$  and  $N_b$  denote their corresponding  $\varepsilon$ -approximation networks, respectively. Let  $F_{a,b}$  be the Fisher Information Matrix of  $N_a$  with the dataset  $X_b^{(2)}$  from the task  $b$ , and  $F_{b,b}$  be the Fisher Information Matrix of  $N_b$  with the dataset  $X_b^{(2)}$  from the task  $b$ . We define the FTD from the task  $a$  to the task  $b$  based on Fréchet distance as follows:*

$$d[a, b] = \frac{1}{\sqrt{2}} \text{tr} \left( F_{a,b} + F_{b,b} - 2(F_{a,b} F_{b,b})^{1/2} \right)^{1/2}, \quad (3)$$

where  $\text{tr}$  denotes the trace of a matrix.

In this paper, we use the diagonal approximation of the Fisher Information matrix since computing the full Fisher matrix is prohibitive in the huge space of neural network parameters. We also normalize them to have a unit trace. As a result, the FTD in (3) can be simplified as follows:

$$\begin{aligned} d[a, b] &= \frac{1}{\sqrt{2}} \left\| F_{a,b}^{1/2} - F_{b,b}^{1/2} \right\|_F \\ &= \frac{1}{\sqrt{2}} \left[ \sum_i \left( (F_{a,b}^{ii})^{1/2} - (F_{b,b}^{ii})^{1/2} \right)^2 \right]^{1/2}, \quad (4) \end{aligned}$$

where  $F^{ii}$  is the  $i^{\text{th}}$  diagonal entry of the Fisher Information matrix. The procedure to compute the FTD is given by Algorithm 1. The FTD ranges from 0 to 1, with the distance  $d = 0$

---

<sup>1</sup>We use  $F$  instead of  $\hat{F}$  onward for the notation simplicity.

denotes a perfect similarity and the distance  $d = 1$  indicates a perfect dissimilarity. As equation (4) shows, the FTD is *asymmetric*. This aligns with human’s common sense that it is often easier to transfer knowledge of a complex task to a simple task than vice versa. Note that the FTD depends on the choice of the  $\varepsilon$ -approximation networks. That is, by using different network architectures to represent the tasks, the computed task distance can be different. This is similar to the human being’s perception: Two people can provide different values of the distance between two tasks. However, it is not likely that their perceptions are different. For instance, people can give different values on the similarity between cat and tiger, but they agree that both cat and tiger are much different from car or plane. In the first part of our experiments, we empirically show this intuition and illustrate that although the computed distances may be different due to the choice of  $\varepsilon$ -approximation networks, the trend of these distances remains consistent across different architectures.

**Definition 4** (Structurally-Similar  $\varepsilon$ -approximation Networks w.r.t.  $(T, X)$ ). *Two  $\varepsilon$ -approximation networks  $N_1$  and  $N_2$  are called structurally-similar w.r.t.  $(T, X)$  if they have exact architecture (the same number of units, the same number of layers, etc), and they are trained on task  $T$  using the training dataset  $X^{(1)}$ .*

Next, we present some theoretical justification for our measure of task similarity. All the proofs are provided in the appendix. Firstly, if we train any pair of structurally-similar  $\varepsilon$ -approximation networks w.r.t some target  $(T, X)$  with the same conditions (e.g., initialization, batch order), the FTD between this pair of networks using the test dataset  $X^{(2)}$  is zero. Formally, we have the following proposition:

**Proposition 1.** *Let  $X$  be the dataset for the target task  $T$ . For any pair of structurally-similar  $\varepsilon$ -approximation networks w.r.t  $(T, X)$  using the full or stochastic gradient descent algorithm with the same initialization settings, learning rate, and the same order of data batches in each epoch for the SGD algorithm, the Fisher task distance between the above pair of  $\varepsilon$ -approximation networks is always zero.*

In this proposition, all the training settings were assumed to be the same for two structurally-similar  $\varepsilon$ -approximation networks w.r.t  $(T, X)$ . However, an important question is whether the FTD is still a *well-defined* measure regardless of the initial settings, learning rate, and the order of data batches. That is, if we train two structurally-similar  $\varepsilon$ -approximation networks w.r.t  $(T, X)$  using SGD with different settings, will the FTD between  $N_1$  and  $N_2$ , as defined in Equation (4), be (close) zero? We answer this question affirmatively assuming a strongly convex loss function. To this end, we invoke Polyak and Juditsky (1992) theorem on the convergence of the average sequence of estimation in different epochs from the SGD algorithm. While the loss function in a deep neural network is not a strongly convex function, establishing the fact that the FTD is mathematically well-defined even for this case is an important step towards the more general case in a deep neural network and a justification for the success of our empirical study. In addition, there are some recent works that try to establish Polyak and Juditsky (1992) theorem for the

convex or even some non-convex functions in an (non)-asymptotic way (Gadat and Panloup 2017). Here, we rely only on the asymptotic version of the theorem proposed originally by Polyak and Juditsky (1992). We first recall the definition of the strongly convex function.

**Definition 5** (Strongly Convex Function). *A differentiable function  $f : \mathbb{R}^n \rightarrow \mathbb{R}$  is strongly convex if for all  $x, y \in \mathbb{R}^n$  and some  $\mu > 0$ ,  $f$  satisfies the following inequality:*

$$f(y) \geq f(x) + \nabla(f)^T(y - x) + \mu\|y - x\|_2^2. \quad (5)$$

Through this paper, we denote  $\ell_\infty$ -norm of a matrix  $B$  as  $\|B\|_\infty = \max_{i,j} |B_{ij}|$ . Also,  $|S|$  means the size of a set  $S$ .

**Theorem 1.** *Let  $X$  be the dataset for the target task  $T$ . Consider  $N_1$  and  $N_2$  as two structurally-similar  $\varepsilon$ -approximation networks w.r.t.  $(T, X)$  respectively with the set of weights  $\theta_1$  and  $\theta_2$  trained using the SGD algorithm where a diminishing learning rate is used for updating weights. Assume that the loss function  $L$  for the task  $T$  is strongly convex, and its 3rd-order continuous derivative exists and bounded. Let the noisy gradient function in training  $N_1$  and  $N_2$  networks using SGD algorithm be given by:*

$$g(\theta_{it}, \epsilon_{it}) = \nabla L(\theta_{it}) + \epsilon_{it}, \quad \text{for } i = 1, 2, \quad (6)$$

where  $\theta_{it}$  is the estimation of the weights for network  $N_i$  at time  $t$ , and  $\nabla L(\theta_{it})$  is the true gradient at  $\theta_{it}$ . Assume that  $\epsilon_{it}$  satisfies  $\mathbb{E}[\epsilon_{it} | \epsilon_{i0}, \dots, \epsilon_{it-1}] = 0$ , and satisfies  $s = \lim_{t \rightarrow \infty} \left\| \left[ \epsilon_{it} \epsilon_{it}^T | \epsilon_{i0}, \dots, \epsilon_{it-1} \right] \right\|_\infty < \infty$  almost surely (a.s.). Then the Fisher task distance between  $N_1$  and  $N_2$  computed on the average of estimated weights up to the current time  $t$  converges to zero as  $t \rightarrow \infty$ . That is,

$$d_t = \frac{1}{\sqrt{2}} \left\| \bar{F}_1^{1/2} - \bar{F}_2^{1/2} \right\|_F \xrightarrow{\mathcal{D}} 0, \quad (7)$$

where  $\bar{F}_i = F(\bar{\theta}_i)$  with  $\bar{\theta}_i = \frac{1}{t} \sum_t \theta_{it}$ , for  $i = 1, 2$ .

In our experiments, we found out that the weights averages  $\bar{\theta}_i$ ,  $i = 1, 2$  can be replaced with only their best estimates for  $\theta_{it}$ ,  $i = 1, 2$ , respectively. Next, we show that the FTD is also a *well-defined* measure between two task-data set pairs. In other words, the (asymmetric) FTD from the task  $(T_A, X_A)$  to the task  $(T_B, X_B)$  approaches a constant value regardless of the initialization, learning rate, and the order of data batches in the SGD algorithm provided that  $X_A$  and  $X_B$  have the same distribution.

**Theorem 2.** *Let  $X_A$  be the dataset for the task  $T_A$  with the objective function  $L_A$ , and  $X_B$  be the dataset for the task  $T_B$  with the objective function  $L_B$ . Assume  $X_A$  and  $X_B$  have the same distribution. Consider an  $\varepsilon$ -approximation network  $N$  trained using both datasets  $X_A^{(1)}$  and  $X_B^{(1)}$  respectively with the objective functions  $L_A$  and  $L_B$  to result weights  $\theta_{At}$  and  $\theta_{Bt}$  at time  $t$ . Under the same assumptions on the moment of gradient noise in SGD algorithm and the loss function stated in Theorem 1, the FTD from the task  $A$  to the task  $B$  computed from the Fisher Information matrices of the average of estimated weights up to the current time  $t$  converges to a constant as  $t \rightarrow \infty$ . That is,*

$$d_t = \frac{1}{\sqrt{2}} \left\| \bar{F}_{A_t}^{1/2} - \bar{F}_{B_t}^{1/2} \right\|_F \xrightarrow{\mathcal{D}} \frac{1}{\sqrt{2}} \left\| F_A^{*1/2} - F_B^{*1/2} \right\|_F, \quad (8)$$

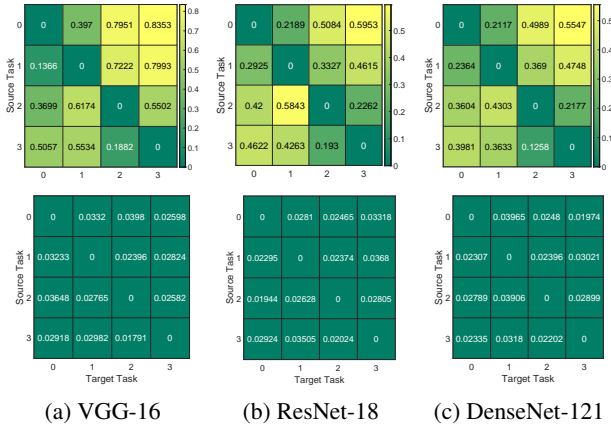


Figure 1: Distance from source tasks to the target tasks on MNIST. The top row shows the mean values and the bottom row denotes the standard deviation of distances between classification tasks over 10 different trials.

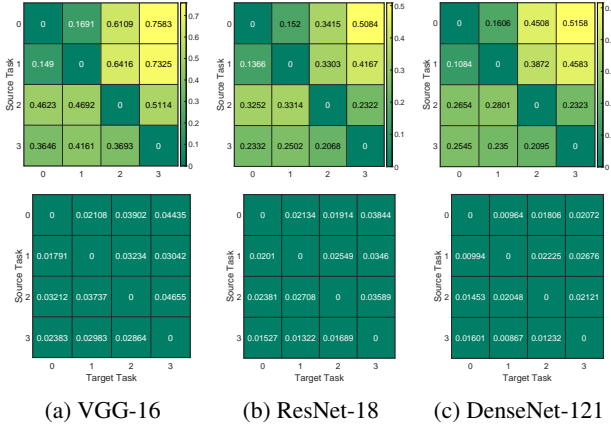


Figure 2: Distance from source tasks to the target tasks on CIFAR-10. The top row shows the mean values and the bottom row denotes the standard deviation of distances between classification tasks over 10 different trials.

where  $\bar{F}_{A_t}$  is given by  $\bar{F}_{A_t} = F(\bar{\theta}_{A_t})$  with  $\bar{\theta}_{A_t} = \frac{1}{t} \sum_t \theta_{A_t}$ , and  $\bar{F}_{B_t}$  is defined in a similar way.

## Experimental Study

In this section, we conduct experiments to show the consistency of our Fisher task distance (FTD), as well as its applications in transfer learning (TL) and neural architecture search (NAS).

### Fisher Task Distance (FTD) Consistency

In this experiment, we show the stability of the FTD by applying our distance on various classification tasks in MNIST, CIFAR-10, CIFAR-100, and ImageNet datasets with different  $\varepsilon$ -approximation networks. For each dataset, we define 4 classification tasks, all of which are variations of the full class classification task. For each task, we consider a

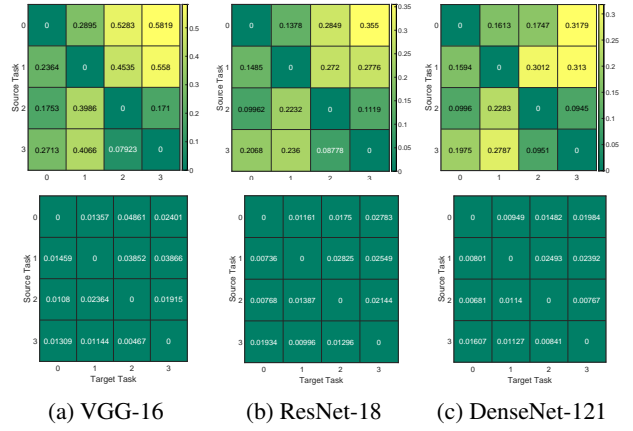


Figure 3: Distance from source tasks to the target tasks on CIFAR-100. The top row shows the mean values and the bottom row denotes the standard deviation of distances between classification tasks over 10 different trials.

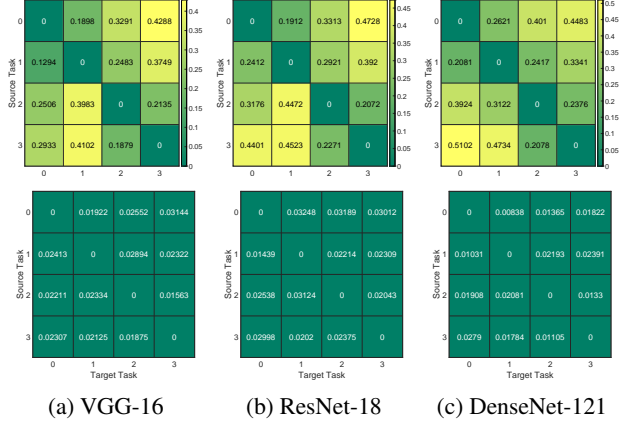


Figure 4: Distance from source tasks to the target tasks on ImageNet. The top row shows the mean values and the bottom row denotes the standard deviation of distances between classification tasks over 10 different trials.

balanced training dataset. That is, except for the classification tasks with all the labels, only a subset of the original training dataset is used such that the number of training samples across all the class labels to be equal. Additionally, we use 3 widely-used and high-performance architectures as the  $\varepsilon$ -approximation networks, including VGG-16 (Simonyan and Zisserman 2014), ResNet-18 (He et al. 2016), DenseNet-121 (Huang et al. 2017). To make sure that our results are statistically significant, we run our experiments 10 times with each of the  $\varepsilon$ -approximation networks being initialized with a different random seed each time and report the mean and the standard deviation of the computed distance.

**MNIST** We define 4 tasks on the MNIST dataset. Task 0 and 1 are the binary classification tasks of detecting digits 0 and 6, respectively. Task 2 is a 5-class classification of detecting digits 0, 1, 2, 3, and anything else. Task 3 is the

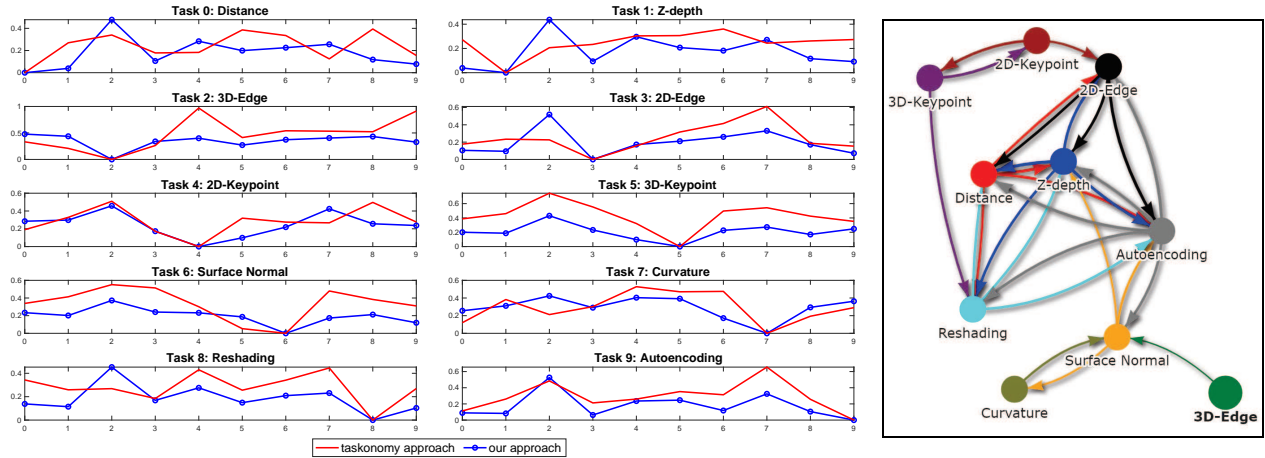


Figure 5: The left panel shows the comparison of task affinity between our approach and Taskonomy (Zamir et al. 2018) approach for each task. The atlas plot of tasks (right panel) found from our approach indicates the computed relationship between tasks according to locations in space.

full 10 digits classification. Figure 1 illustrates the mean and standard deviation of the distances between each pair of tasks after 10 runs using 3 different architectures. The columns of the tables denote the distance to the target task and the rows represent the distance from the source tasks. Our results suggest that Task 0 and 1 are highly related, and Task 3 is the closest task to Task 2. Moreover, the relation between tasks remain the same regardless of choosing  $\varepsilon$ -approximation networks.

**CIFAR-10** We define 4 tasks in the CIFAR-10 dataset. Task 0 is a binary classification of indicating 3 objects: automobile, cat, ship (i.e., the goal is to decide if the given input image consists of one of these three objects or not). Task 1 is analogous to Task 0 but with different objects: cat, ship, truck. Task 2 is a 4-class classification with labels bird, frog, horse, and anything else. Task 3 is the standard 10 objects classification. Figure 2 illustrates the mean and standard deviation of the distance between CIFAR-10 tasks over 10 trial runs, using 3 different architectures. As we can see in Figures 2, the closest tasks to target tasks in all the tables always result in a unique task no matter what  $\varepsilon$ -approximation network we choose. Additionally, in Figure 7 (in the appendix), we study the effect of different initial settings, such as training with/without data augmentation, or using unbalanced data set for the above 4 tasks on the CIFAR-10 data set and using VGG-16 as the  $\varepsilon$ -approximation network. Again the same conclusion about the consistency of the FTD holds.

**CIFAR-100** We define 4 tasks in the CIFAR-100 dataset, consisting of 100 objects equally distributed in 20 sub-classes, each sub-class has 5 objects. We define Task 0 as a binary classification of detecting an object that belongs to vehicles 1 and 2 sub-classes or not (i.e., the goal is to decide if the given input image consists of one of these 10 vehicles or not). Task 1 is analogous to Task 0 but with different sub-classes: household furniture and devices. Task 2 is a multi-classification with 11 labels defined on vehicles 1, vehicles 2, and anything else. Finally, Task 3 is defined similarly to

Task 2; however, with the 21-labels in vehicles 1, vehicles 2, household furniture, household device, and anything else. Figure 3 illustrates the mean and the standard deviation of the distance between CIFAR-100 tasks after 10 runs using 3 different  $\varepsilon$ -approximation networks. Here, the closest tasks to any target tasks are distinctive regardless of the choice of the  $\varepsilon$ -approximation network.

**ImageNet** Finally, we define four 10-class classification tasks in ImageNet dataset. For each class, we consider 800 for training and 200 for the test samples. The list of 10 classes in Task 0 includes tench, English springer, cassette player, chain saw, church, French horn, garbage truck, gas pump, golf ball, parachute. Task 1 is similar to Task 0; however, instead of 3 labels of tench, golf ball, and parachute, it has samples from the grey whale, volleyball, umbrella classes. In Task 2, we also replace 5 labels of grey whale, cassette player, chain saw, volleyball, umbrella in Task 0 with another 5 labels given by platypus, laptop, lawnmower, baseball, cowboy hat. Lastly, Task 3 is defined as a 10-class classification task with samples from the following classes: analog clock, candle, sweatshirt, birdhouse, ping-pong ball, hotdog, pizza, school bus, iPod, beaver. The mean and standard deviation tables of the distances between ImageNet tasks for 10 trials with 3  $\varepsilon$ -approximation networks are illustrated in Figure 4. Again, it is observed that the order of the distance between the source and target tasks remains the same independent of the  $\varepsilon$ -approximation networks.

Overall, although the value of task distance depends on the  $\varepsilon$ -approximation network, the trend remains the same across all 3 architectures. In addition, the standard deviation values in the bottom row of the figures suggest that the computed task distance is stable as the fluctuations over the mean values do not show any overlap with each other.

### Application in Transfer Learning

We now show the application of the FTD in transfer learning by comparing the task affinity found using our task dis-

tance with the brute-force method proposed by Zamir et al. (2018) on the Taskonomy dataset. The Taskonomy dataset is a collection of  $512 \times 512$  colorful images of varied indoor scenes. It provides the pre-processed ground truth for 25 vision tasks including semantic and low-level tasks. In this experiment, we consider a set of 10 visual tasks, including: (0) Euclidean distance, (1) z-depth, (2) 3D-edge, (3) 2D-edge (4) 2D-keypoint, (5) 3D-keypoint, (6) surface normal, (7) curvature, (8) reshading, (9) autoencoding. Please see (Zamir et al. 2018) for detailed task descriptions. Each task has 40,000 training samples and 10,000 test samples. A deep autoencoder architecture, including convolutional and linear layers, with a total of 50.51M parameters, is chosen to be the  $\varepsilon$ -approximation network for all visual tasks.

In order to use the autoencoder for all the visual tasks without architecture modification, we convert all of the ground truth outputs to three channels. Figure 8 in the appendix shows the mean (top panel) and the standard deviation (middle panel) of the task distance between each pair of tasks over 10 different initial settings in the training of the  $\varepsilon$ -approximation network. The bottom panel shows the task affinity achieved by the brute-force method from the Taskonomy paper for only a single run. Note that, the task affinities are asymmetric (or non-commutative) in both approaches. The task affinity found by the brute-force approach requires a lot more computations, and does not give a clear boundary between tasks (e.g., difficult to identify the closest tasks to some target tasks). Our approach, on the other hand, is statistical and determines a clear boundary for the identification of related tasks based on the distance. The left panel of Figure 5 illustrates the comparison of task affinity by our approach and by the brute-force approach in the Taskonomy paper. We note that both approaches follow a similar trend for most of the tasks. The right panel of Figure 5 shows the atlas plot of tasks found by our approach, which represents the relationship of tasks according to the location in space. Overall, our FTD is capable of identifying the related tasks with clear statistical boundaries between tasks (i.e., low standard deviation) while requiring significantly less computational resources compared to the brute-force approach (with less statistical significance) in the Taskonomy paper. Thus, the FTD can be applied to quickly solve the TL problems.

### Application in Neural Architecture Search

In this section, we apply Fisher task distance to the task-aware neural architecture search (TA-NAS) framework (Le et al. 2021), which finds the suitable architecture for a target task, based on a set of baseline tasks. Consider a set  $A$  consisting of  $K$  baseline tasks  $T_i$  and its corresponding data set  $X_i$ , denoted jointly by pairs  $(T_i, X_i)$  for  $i = 1, 2, \dots, K$ . Below, TA-NAS framework with the FTD is presented for finding a well-performing architecture for a target task  $b$ , denoted by the pair  $(T_b, X_b)$ , based on the knowledge of architectures of these  $K$  learned baseline tasks. We assume that  $X_1, X_2, \dots, X_K$  and  $X_b$  are known, and their data points are of the same dimension. The pipeline of the TA-NAS, whose pseudo-code is given by Algorithm 2, is summarized below:

1. **Fisher Task Distance.** First, the FTD of each learned

---

### Algorithm 2: TA-NAS framework

---

**Data:**  $A = \{(T_1, X_1), \dots, (T_K, X_K)\}$ ,  $b = (T_b, X_b)$

**Input:**  $\varepsilon$ -approx. network  $N$ , # of candidates  $C$ ,  
 $\alpha = 1/|C|$ , baseline spaces  $\{S_1, \dots, S_K\}$

**Output:** Best architecture for  $b$

```

1 Function FUSE (candidates  $C$ , data  $X$ ) :
2   Relax the output of  $C$  (using Softmax function):
   
$$\bar{c}(X) = \sum_{c \in C} \frac{\exp(\alpha c)}{\sum_{c' \in C} \exp(\alpha c')} c(X)$$

3   while  $\alpha$  not converge do
4     Update  $C$  by descending  $\nabla_w \mathcal{L}_{tr}(w; \alpha, \bar{c})$ 
5     Update  $\alpha$  by descending  $\nabla_\alpha \mathcal{L}_{val}(\alpha; w, \bar{c})$ 
6   return  $c^* = \operatorname{argmin}_{c \in C} \alpha_c$ 

7 Function Main:
8   for  $a \in A$  do
9     Compute Fisher Task Distance from  $a$  to  $b$ :
10     $d[a, b] = \text{TaskDistance}(X_a^{(1)}, X_b, N)$ 
11    Select closest task:  $a^* = \operatorname{argmin}_{a \in A} d[a, b]$ 
12    Define search space  $S = S_{a^*}$ 
13    while criteria not met do
14      Sample  $C$  candidates  $\in S$ 
15       $c^* = \text{FUSE}((C \cup c^*), X_b)$ 
16    return best architecture  $c^*$ 

```

---

baseline task  $a \in A$  to the target task  $b$  is computed. The closest baseline task  $a^*$ , based on the computed distances, is returned.

2. **Neural Architecture Search.** Next, a suitable search space for the target task  $b$  is determined based on the closest task architecture. Finally, the FUSE algorithm (Le et al. 2021) performs a search within this space to find a well-performing architecture for the target task  $b^2$ .

In TA-NAS, the architecture search space for a target task is restricted only to the space of the most related task from the baseline tasks. Thus, the search algorithm performs efficiently and requires fewer computational resources as it is demonstrated in our experiments on classification tasks in MNIST, CIFAR-10, CIFAR-100, ImageNet datasets.

**MNIST** We consider the problem of learning architecture for the target Task 2 of MNIST dataset, using the other aforementioned tasks as our baseline tasks. It is observed in Figure 1 that Task 3 is the closest one to Task 2. As the result, we apply cell structure and the operations of Task 3 to generate a suitable search space for the target task. The results in Table 1 show the best test accuracy of the optimal architecture found by our method compared to well-known handcrafted networks (i.e., VGG-16, ResNet-18, DenseNet-121), the state-of-the-art NAS methods (i.e., random search

---

<sup>2</sup>A discussion of FUSE algorithm is provided in the appendix.

Table 1: Comparison of our TA-NAS framework with the hand-designed image classifiers, and state-of-the-art NAS methods on Task 2 (binary classification) of MNIST.

Architecture	Accuracy	No. Params. (M)	GPU days
VGG-16	99.41	14.72	-
ResNet-18	99.47	11.44	-
DenseNet-121	99.61	6.95	-
Random Search	99.52	2.12	5
ENAS (1st)	94.29	4.60	2
ENAS (2nd)	94.71	4.60	4
DARTS (1st)	98.82	2.17	2
DARTS (2nd)	99.44	2.23	4
PC-DARTS (1st)	98.76	1.78	2
PC-DARTS (2nd)	99.88	2.22	4
TE-NAS	99.71	2.79	2
<b>TA-NAS (ours)</b>	<b>99.86</b>	<b>2.14</b>	<b>2</b>

Table 2: Comparison of our TA-NAS framework with the hand-designed image classifiers, and state-of-the-art NAS methods on Task 2 (11-class classification) of CIFAR-100.

Architecture	Accuracy	No. Params. (M)	GPU days
VGG-16	83.93	14.72	-
ResNet-18	84.56	11.44	-
DenseNet-121	88.47	6.95	-
Random Search	88.55	3.54	5
ENAS	10.49	4.60	4
DARTS	87.57	3.32	4
PC-DARTS	85.36	2.43	4
TE-NAS	88.92	3.66	4
<b>TA-NAS (ours)</b>	<b>90.96</b>	<b>3.17</b>	<b>4</b>

algorithm (Li and Talwalkar 2020), ENAS (Pham et al. 2018), DARTS (Liu, Simonyan, and Yang 2018), PC-DARTS (Xu et al. 2019), TE-NAS (Chen, Gong, and Wang 2021)). The architecture discovered by our method is competitive with these networks while it results in a significantly smaller amount of parameters and GPU days.

**CIFAR-10/100** We consider the problem of searching for a high-performing and efficient architecture for Task 2 in CIFAR-10, and Task 2 in CIFAR-100 datasets. As observed in Figure 2 and Figure 3, we consider Task 3 as the closest task for both cases. Results in Table 3 and 2 suggest that our constructed architectures for these tasks have higher test accuracy with a fewer number of parameters and GPU days compared to other approaches. The poor performance of ENAS in CIFAR-100 highlights the lack of robustness of this method since its search space is defined to only for full class classification in CIFAR-10.

**ImageNet** We consider Task 1 in ImageNet dataset as the target task. Based on the computed distances in Figure 4, we use Task 0 as the closest source task to our target task.

Table 3: Comparison of our TA-NAS framework with the hand-designed image classifiers, and state-of-the-art NAS methods on Task 2 (4-class classification) of CIFAR-10.

Architecture	Accuracy	No. Params. (M)	GPU days
VGG-16	86.75	14.72	-
ResNet-18	86.93	11.44	-
DenseNet-121	88.12	6.95	-
Random Search	88.55	3.65	5
ENAS (1st)	73.23	4.60	2
ENAS (2nd)	75.22	4.60	4
DARTS (1st)	90.11	3.12	2
DARTS (2nd)	91.19	3.28	4
PC-DARTS (1st)	92.07	3.67	2
PC-DARTS (2nd)	92.49	3.66	4
TE-NAS	91.02	3.78	2
<b>TA-NAS (ours)</b>	<b>92.58</b>	<b>3.13</b>	<b>2</b>

Table 4: Comparison of our TA-NAS framework with the hand-designed image classifiers, and state-of-the-art NAS methods on Task 1 (10-class classification) of ImageNet.

Architecture	Accuracy	No. Params. (M)	GPU days
VGG-16	89.88	14.72	-
ResNet-18	91.14	11.44	-
DenseNet-121	94.76	6.95	-
Random Search	95.02	3.78	5
ENAS	33.65	4.60	4
DARTS	95.22	3.41	4
PC-DARTS	88.00	1.91	4
TE-NAS	95.37	4.23	4
<b>TA-NAS (ours)</b>	<b>95.92</b>	<b>3.43</b>	<b>4</b>

Table 4 presents results indicating that our model has higher test accuracy with a fewer number of parameters compared to other approaches. In complex datasets (e.g., CIFAR-100, ImageNet), the method with fixed search space (i.e., ENAS) is only capable of finding architectures for tasks in standard datasets, performs poorly compared with other methods in our benchmark. Our experiments suggest that the proposed framework can utilize the knowledge of the most similar task in order to find a high-performing architecture for the target task with a fewer number of parameters.

## Conclusions

A task similarity measure based on the Fisher Information matrix has been introduced in this paper. This non-commutative measure called Fisher Task distance (FTD), represents the complexity of applying the knowledge of one task to another. The theory and experimental experiments demonstrate that the distance is consistent and well-defined. In addition, two applications of FTD, including transfer learning and NAS has been investigated. In particular, the task affinity results found using this measure is well-aligned



with the result found using the traditional transfer learning approach. Moreover, the FTD is applied in NAS to define a reduced search space of architectures for a target task. This reduces the complexity of the architecture search, increases its efficiency, and leads to superior performance with a smaller number of parameters.

## Acknowledgments

This work was supported by the Army Research Office grant No. W911NF-15-1-0479.

## References

- Achille, A.; Lam, M.; Tewari, R.; Ravichandran, A.; Maji, S.; Fowlkes, C.; Soatto, S.; and Perona, P. 2019. Task2Vec: Task Embedding for Meta-Learning. *arXiv e-prints*, arXiv:1902.03545.
- Awad, N.; Mallik, N.; and Hutter, F. 2020. Differential Evolution for Neural Architecture Search. *arXiv preprint arXiv:2012.06400*.
- Bender, G.; Kindermans, P.-J.; Zoph, B.; Vasudevan, V.; and Le, Q. 2018. Understanding and simplifying one-shot architecture search. *Proc. Int. Conf. Machine Learning*.
- Bender, G.; Liu, H.; Chen, B.; Chu, G.; Cheng, S.; Kindermans, P.-J.; and Le, Q. V. 2020. Can weight sharing outperform random architecture search? an investigation with tunas. In *Proceedings of the IEEE/CVF Conference on Computer Vision and Pattern Recognition*, 14323–14332.
- Cai, H.; Chen, T.; Zhang, W.; Yu, Y.; and Wang, J. 2018. Efficient architecture search by network transformation. *Proc. Assoc. Adv. Art. Intell. (AAAI)*.
- Cai, H.; Gan, C.; Wang, T.; Zhang, Z.; and Han, S. 2019. Once-for-all: Train one network and specialize it for efficient deployment. *arXiv preprint arXiv:1908.09791*.
- Cai, H.; Zhu, L.; and Han, S. 2019. ProxylessNAS: Direct neural architecture search on target task and hardware. *Proc. Int. Conf. Learning Representations*.
- Chen, S.; Zhang, C.; and Dong, M. 2018. Coupled end-to-end transfer learning with generalized fisher information. In *Proceedings of the IEEE Conference on Computer Vision and Pattern Recognition*, 4329–4338.
- Chen, W.; Gong, X.; and Wang, Z. 2021. Neural Architecture Search on ImageNet in Four GPU Hours: A Theoretically Inspired Perspective. *arXiv preprint arXiv:2102.11535*.
- Cho, M.; Soltani, M.; and Hegde, C. 2019. One-shot neural architecture search via compressive sensing. *arXiv preprint arXiv:1906.02869*.
- Dong, X.; and Yang, Y. 2020. Nas-bench-102: Extending the scope of reproducible neural architecture search. *arXiv preprint arXiv:2001.00326*.
- Dwivedi, K.; and Roig, G. 2019. Representation Similarity Analysis for Efficient Task Taxonomy and Transfer Learning. In *CVPR*. IEEE Computer Society.
- Elsken, T.; Metzen, J. H.; and Hutter, F. 2019. Efficient Multi-objective Neural Architecture Search via Lamarckian Evolution. *Proc. Int. Conf. Learning Representations*.
- Finn, C.; Tan, X. Y.; Duan, Y.; Darrell, T.; Levine, S.; and Abbeel, P. 2016. Deep spatial autoencoders for visuomotor learning. In *Robotics and Automation (ICRA), 2016 IEEE International Conference on*, 512–519. IEEE.
- Gadat, S.; and Panloup, F. 2017. Optimal non-asymptotic bound of the Ruppert-Polyak averaging without strong convexity. *arXiv preprint arXiv:1709.03342*.
- He, C.; Ye, H.; Shen, L.; and Zhang, T. 2020. Milenas: Efficient neural architecture search via mixed-level reformulation. In *Proceedings of the IEEE/CVF Conference on Computer Vision and Pattern Recognition*, 11993–12002.
- He, K.; Zhang, X.; Ren, S.; and Sun, J. 2016. Deep residual learning for image recognition. *IEEE Conf. Comp. Vision and Pattern Recog.*
- Hu, H.; Langford, J.; Caruana, R.; Mukherjee, S.; Horvitz, E.; and Dey, D. 2019. Efficient Forward Architecture Search. *Adv. Neural Inf. Proc. Sys. (NeurIPS)*.
- Huang, G.; Liu, Z.; Van Der Maaten, L.; and Weinberger, K. Q. 2017. Densely connected convolutional networks. *IEEE Conf. Comp. Vision and Pattern Recog.*
- Jin, H.; Song, Q.; and Hu, X. 2018. Efficient neural architecture search with network morphism. *arXiv preprint arXiv:1806.10282*.
- Kingma, D. P.; and Ba, J. 2014. Adam: A method for stochastic optimization. *arXiv preprint arXiv:1412.6980*.
- Kirkpatrick, J.; Pascanu, R.; Rabinowitz, N.; Veness, J.; Desjardins, G.; Rusu, A. A.; Milan, K.; Quan, J.; Ramalho, T.; Grabska-Barwinska, A.; et al. 2017. Overcoming catastrophic forgetting in neural networks. *Proceedings of the national academy of sciences*, 114(13): 3521–3526.
- Krizhevsky, A.; Hinton, G.; et al. 2009. Learning multiple layers of features from tiny images. *Citeseer*.
- Le, C. P.; Soltani, M.; Ravier, R.; and Tarokh, V. 2021. Task-aware neural architecture search. In *ICASSP 2021-2021 IEEE International Conference on Acoustics, Speech and Signal Processing (ICASSP)*, 4090–4094. IEEE.
- LeCun, Y.; Cortes, C.; and Burges, C. 2010. MNIST handwritten digit database. *AT&T Labs [Online]*. Available: <http://yann.lecun.com/exdb/mnist>, 2: 18.
- Li, L.; Jamieson, K.; Rostamizadeh, A.; Gonina, E.; Hardt, M.; Recht, B.; and Talwalkar, A. 2018. Massively parallel hyperparameter tuning. *arXiv preprint arXiv:1810.05934*.
- Li, L.; and Talwalkar, A. 2020. Random search and reproducibility for neural architecture search. In *Uncertainty in artificial intelligence*, 367–377. PMLR.
- Liu, C.; Zoph, B.; Neumann, M.; Shlens, J.; Hua, W.; Li, L.-J.; Fei-Fei, L.; Yuille, A.; Huang, J.; and Murphy, K. 2018. Progressive neural architecture search. *Euro. Conf. Comp. Vision*.
- Liu, H.; Simonyan, K.; and Yang, Y. 2018. Darts: Differentiable architecture search. *Proc. Int. Conf. Machine Learning*.
- Luo, R.; Tian, F.; Qin, T.; Chen, E.; and Liu, T.-Y. 2018. Neural architecture optimization. *Adv. Neural Inf. Proc. Sys. (NeurIPS)*.



- Luo, Z.; Zou, Y.; Hoffman, J.; and Fei-Fei, L. F. 2017. Label Efficient Learning of Transferable Representations across Domains and Tasks. In *Advances in Neural Information Processing Systems*, 164–176.
- Mihalkova, L.; Huynh, T.; and Mooney, R. J. 2007. Mapping and revising Markov logic networks for transfer learning. In *AAAI*, volume 7, 608–614.
- Nguyen, V.; Le, T.; Yamada, M.; and Osborne, M. A. 2020. Optimal transport kernels for sequential and parallel neural architecture search. *arXiv preprint arXiv:2006.07593*.
- Niculescu-Mizil, A.; and Caruana, R. 2007. Inductive transfer for Bayesian network structure learning. In *Artificial Intelligence and Statistics*, 339–346.
- Noy, A.; Nayman, N.; Ridnik, T.; Zamir, N.; Doveh, S.; Friedman, I.; Giryas, R.; and Zelnik-Manor, L. 2019. ASAP: Architecture search, anneal and prune. *arXiv preprint arXiv:1904.04123*.
- Pal, A.; and Balasubramanian, V. N. 2019. Zero-Shot Task Transfer. *arXiv:1903.01092*.
- Pan, S. J.; and Yang, Q. 2010. A Survey on Transfer Learning. *IEEE Transactions on Knowledge and Data Engineering*, 22(10): 1345–1359.
- Pham, H.; Guan, M. Y.; Zoph, B.; Le, Q. V.; and Dean, J. 2018. Efficient neural architecture search via parameter sharing. *Proc. Int. Conf. Machine Learning*.
- Polyak, B.; and Juditsky, A. 1992. Acceleration of stochastic approximation by averaging. *Siam Journal on Control and Optimization*, 30: 838–855.
- Razavian, A. S.; Azizpour, H.; Sullivan, J.; and Carlsson, S. 2014. CNN Features Off-the-Shelf: An Astounding Baseline for Recognition. In *Proceedings of the 2014 IEEE Conference on Computer Vision and Pattern Recognition Workshops*, CVPRW '14, 512–519. Washington, DC, USA: IEEE Computer Society. ISBN 978-1-4799-4308-1.
- Real, E.; Aggarwal, A.; Huang, Y.; and Le, Q. V. 2019. Regularized evolution for image classifier architecture search. *Proc. Assoc. Adv. Art. Intell. (AAAI)*.
- Russakovsky, O.; Deng, J.; Su, H.; Krause, J.; Satheesh, S.; Ma, S.; Huang, Z.; Karpathy, A.; Khosla, A.; Bernstein, M.; Berg, A. C.; and Fei-Fei, L. 2015. ImageNet Large Scale Visual Recognition Challenge. *International Journal of Computer Vision (IJCV)*, 115(3): 211–252.
- Sciuto, C.; Yu, K.; Jaggi, M.; Musat, C.; and Salzmann, M. 2019. Evaluating the Search Phase of Neural Architecture Search. *arXiv preprint arXiv:1902.08142*.
- Silver, D. L.; and Bennett, K. P. 2008. Guest editor’s introduction: special issue on inductive transfer learning. *Machine Learning*, 73(3): 215–220.
- Simonyan, K.; and Zisserman, A. 2014. Very deep convolutional networks for large-scale image recognition. *arXiv preprint arXiv:1409.1556*.
- Song, X.; Choromanski, K.; Parker-Holder, J.; Tang, Y.; Peng, D.; Jain, D.; Gao, W.; Pacchiano, A.; Sarlos, T.; and Yang, Y. 2021. ES-ENAS: Combining Evolution Strategies with Neural Architecture Search at No Extra Cost for Reinforcement Learning. *arXiv preprint arXiv:2101.07415*.
- Standley, T.; Zamir, A.; Chen, D.; Guibas, L.; Malik, J.; and Savarese, S. 2020. Which Tasks Should Be Learned Together in Multi-task Learning? In III, H. D.; and Singh, A., eds., *Proceedings of the 37th International Conference on Machine Learning*, volume 119 of *Proceedings of Machine Learning Research*, 9120–9132. PMLR.
- Sun, Y.; Sun, X.; Fang, Y.; Yen, G. G.; and Liu, Y. 2021. A Novel Training Protocol for Performance Predictors of Evolutionary Neural Architecture Search Algorithms. *IEEE Transactions on Evolutionary Computation*, 1–1.
- Wan, A.; Dai, X.; Zhang, P.; He, Z.; Tian, Y.; Xie, S.; Wu, B.; Yu, M.; Xu, T.; Chen, K.; et al. 2020. Fbnetv2: Differentiable neural architecture search for spatial and channel dimensions. In *Proceedings of the IEEE/CVF Conference on Computer Vision and Pattern Recognition*, 12965–12974.
- Wang, A. Y.; Wehbe, L.; and Tarr, M. J. 2019. Neural Taskonomy: Inferring the Similarity of Task-Derived Representations from Brain Activity. *BioRxiv*, 708016.
- Xie, S.; Zheng, H.; Liu, C.; and Lin, L. 2018. SNAS: stochastic neural architecture search. *arXiv preprint arXiv:1812.09926*.
- Xu, Y.; Xie, L.; Zhang, X.; Chen, X.; Qi, G.-J.; Tian, Q.; and Xiong, H. 2019. PC-DARTS: Partial channel connections for memory-efficient architecture search. *arXiv preprint arXiv:1907.05737*.
- Yang, Z.; Wang, Y.; Chen, X.; Shi, B.; Xu, C.; Xu, C.; Tian, Q.; and Xu, C. 2020. Cars: Continuous evolution for efficient neural architecture search. In *Proceedings of the IEEE/CVF Conference on Computer Vision and Pattern Recognition*, 1829–1838.
- Zamir, A. R.; Sax, A.; Shen, W. B.; Guibas, L.; Malik, J.; and Savarese, S. 2018. Taskonomy: Disentangling Task Transfer Learning. In *2018 IEEE Conference on Computer Vision and Pattern Recognition (CVPR)*. IEEE.
- Zhang, M.; Li, H.; Pan, S.; Chang, X.; and Su, S. 2020. Overcoming multi-model forgetting in one-shot nas with diversity maximization. In *Proceedings of the IEEE/CVF Conference on Computer Vision and Pattern Recognition*, 7809–7818.
- Zhao, Y.; Wang, L.; Tian, Y.; Fonseca, R.; and Guo, T. 2020. Few-shot neural architecture search. *arXiv preprint arXiv:2006.06863*.
- Zhou, D.; Zhou, X.; Zhang, W.; Loy, C. C.; Yi, S.; Zhang, X.; and Ouyang, W. 2020. Econas: Finding proxies for economical neural architecture search. In *Proceedings of the IEEE/CVF Conference on Computer Vision and Pattern Recognition*, 11396–11404.
- Zoph, B.; and Le, Q. V. 2017. Neural architecture search with reinforcement learning. *Proc. Int. Conf. Learning Representations*.
- Zoph, B.; Vasudevan, V.; Shlens, J.; and Le, Q. V. 2018. Learning transferable architectures for scalable image recognition. *IEEE Conf. Comp. Vision and Pattern Recog.*

## Appendix

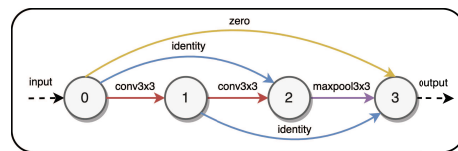
### Detail of Experiments

In our experiments, the first step is represent each task and its corresponding dataset by an  $\varepsilon$ -approximation network. To this end, we train the  $\varepsilon$ -approximation network with the balanced data from each task. For classification tasks (e.g., tasks in MNIST (LeCun, Cortes, and Burges 2010), CIFAR-10 (Krizhevsky, Hinton et al. 2009), CIFAR-100 (Krizhevsky, Hinton et al. 2009), ImageNet (Russakovsky et al. 2015)), three different architectures (e.g., VGG-16 (Simonyan and Zisserman 2014), Resnet-18 (He et al. 2016), DenseNet-121 (Huang et al. 2017)) are chosen as  $\varepsilon$ -approximation network architectures. The training procedure is conducted in 100 epochs, with Adam optimizer (Kingma and Ba 2014), a batch size is set to 128, and cross-validation loss. For image processing tasks in Taskonomy dataset (Zamir et al. 2018), we use an autoencoder as the  $\varepsilon$ -approximation network. The part of the autoencoder consists of one convolutional layer, and two linear layers. The convolutional layer has 3 input channels and 16 output channels with the kernel size equals to 5. We also use the zero padding of size 2, stride of size 4, and dilation equals to 1. The first linear layer has the size of (262144, 512), and the second linear layer has the size of (512, 128). The training procedure is conducted in 20 epochs with Adam optimizer (Kingma and Ba 2014), a batch size of 64, and mean-square error loss.

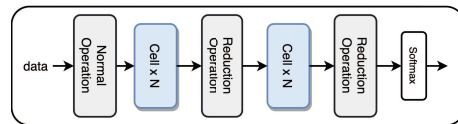
In order to construct the dictionary for baseline tasks, we need to perform the architecture search for these tasks using general search space. This space is defined by cells structure, consisting of 3 or 4 nodes, and 10 operations (i.e., zero, identity, maxpool3x3, avepool3x3, conv3x3, conv5x5, conv7x7, dil-conv3x3, dil-conv5x5, conv7x1-1x7). After the best cell for each baseline task is founded, we save the structures and operations to the dictionary. Next, we apply the task-aware neural architecture search (TA-NAS) framework (Le et al. 2021) to find the best architecture for a target task, given a knowledge of learned baseline tasks.

First, consider a set  $A$  consisting of  $K$  baseline tasks  $T_i$  and its corresponding data set  $X_i$ , denoted jointly by pairs  $(T_i, X_i)$  for  $i = 1, 2, \dots, K$  where  $X_i = X_i^{(1)} \cup X_i^{(2)}$  with  $X_i^{(1)}$  and  $X_i^{(2)}$  denote the training and the test data, respectively. Now, suppose that for a given  $\varepsilon$ , the  $\varepsilon$ -approximation networks for the tasks,  $(T_i, X_i)$  for  $i = 1, 2, \dots, K$  denoted by  $N_1, N_2, \dots, N_k$ , respectively, where  $\varepsilon$  is selected such that  $\min_{i \in \{1, 2, \dots, K\}} \mathcal{P}_{N_i}(T_i, X_i^{(2)}) \geq 1 - \varepsilon$ . Here, the Fisher task distance from each of the baseline tasks to the target is computed. The baseline task with the smallest distance (i.e., the most related task) will be selected and used to construct the restricted search space for the target task. Lastly, the Fusion Search (FUSE) algorithm (Le et al. 2021) is applied to search for the best architecture for the target task from the restricted search space.

The experiment is conducted using NVIDIA GeForce RTX 3090. The source code for the experiments is available at: <https://github.com/lephuoccat/Fisher-Information-NAS>. Next, we provide the detail of the TA-NAS framework.



(a) A cell structure



(b) A skeleton structure

Figure 6: An example of the cell and the skeleton.

### Search Space and Search Algorithm in TA-NAS

In an analogous manner to recent NAS techniques (Liu, Simonyan, and Yang 2018; Dong and Yang 2020), our architecture search space is defined by cells and skeletons. A cell, illustrated in Figure 6a, is a densely connected directed-acyclic graph (DAG) of nodes, where nodes are connected by operations. The operations (e.g., identity, zero, convolution, pooling) are normally set so that the dimension of the output is the same as that of the input. Additionally, a skeleton, illustrated in Figure 6b, is a structure consisting of multiple cells and other operations stacked together, forming a complete architecture. In our framework, the search space for the task is defined in terms of the cells and operations.

For finding the best candidate for the incoming target task, the Fusion Search (FUSE) algorithm is applied to the restricted search space of the closest task. In each iteration, a number of candidate networks are drawn from the search space. Next, an  $\alpha$  coefficient is assigned to the output of each candidate to create the weighted sum output of the candidates. This search algorithm considers all candidates as a whole by relaxing their outputs, and performs the optimization using gradient descent. In other words, it jointly trains the networks' weights and their  $\alpha$  coefficients. After the training procedure, the network with the highest  $\alpha$  coefficient is chosen as the most promising candidate. This process repeats until certain criteria are met.

### Proofs of theorems

Here, we provide the the proof of the proposition 1, the proof of the theorem 1, and the proof of the theorem 2.

**Proposition 1.** *Let  $X$  be the dataset for the target task  $T$ . For any pair of structurally-similar  $\varepsilon$ -approximation network w.r.t  $(T, X)$  using the full or stochastic gradient descent algorithm with the same initialization settings, learning rate, and the same order of data batches in each epoch for the SGD algorithm, the Fisher task distance between the above pair of  $\varepsilon$ -approximation networks is always zero.*

**Proof of Proposition 1.** Let  $N_1$  and  $N_2$  be two structurally-similar  $\varepsilon$ -approximation network w.r.t  $(T, X)$  trained using the full or stochastic gradient descent algorithm. According

to the Definition 4 and assumptions in the proposition, the Fisher Information Matrices of  $N_1$  and  $N_2$  are the same; hence, the Fisher task distance is zero.  $\square$

**Theorem 1.** *Let  $X$  be the dataset for the target task  $T$ . Consider  $N_1$  and  $N_2$  as two structurally-similar  $\varepsilon$ -approximation networks w.r.t.  $(T, X)$  respectively with the set of weights  $\theta_1$  and  $\theta_2$  trained using the SGD algorithm where a diminishing learning rate is used for updating weights. Assume that the loss function  $L$  for the task  $T$  is strongly convex, and its 3rd-order continuous derivative exists and bounded. Let the noisy gradient function in training  $N_1$  and  $N_2$  networks using SGD algorithm be given by:*

$$g(\theta_{it}, \epsilon_{it}) = \nabla L(\theta_{it}) + \epsilon_{it}, \text{ for } i = 1, 2, \quad (9)$$

where  $\theta_{it}$  is the estimation of the weights for network  $N_i$  at time  $t$ , and  $\nabla L(\theta_{it})$  is the true gradient at  $\theta_{it}$ . Assume that  $\epsilon_{it}$  satisfies  $\mathbb{E}[\epsilon_{it} | \epsilon_{i0}, \dots, \epsilon_{it-1}] = 0$ , and satisfies  $s = \lim_{t \rightarrow \infty} \mathbb{E}[\|\epsilon_{it} \epsilon_{it}^T | \epsilon_{i0}, \dots, \epsilon_{it-1}\|] < \infty$  almost surely (a.s.). Then the Fisher task distance between  $N_1$  and  $N_2$  computed on the average of estimated weights up to the current time  $t$  converges to zero as  $t \rightarrow \infty$ . That is,

$$d_t = \frac{1}{\sqrt{2}} \left\| \bar{F}_{1t}^{1/2} - \bar{F}_{2t}^{1/2} \right\|_F \xrightarrow{\mathcal{D}} 0, \quad (10)$$

where  $\bar{F}_{it} = F(\bar{\theta}_{it})$  with  $\bar{\theta}_{it} = \frac{1}{t} \sum_t \theta_{it}$ , for  $i = 1, 2$ .

**Proof of Theorem 1.** Here, we show the proof for the full Fisher Information Matrix; however, the same results holds for the diagonal approximation of the Fisher Information Matrix. Let  $N_1$  with weights  $\theta_1$  and  $N_2$  with weights  $\theta_2$  be the two structurally-similar  $\varepsilon$ -approximation networks w.r.t.  $(T, X)$ . Let  $n$  be the number of trainable parameters in  $N_1$  and  $N_2$ . Since the objective function is strongly convex and the fact that  $N_1$  and  $N_2$  are structurally-similar  $\varepsilon$ -approximation networks w.r.t.  $(T, X)$ , both of these network will obtain the optimum solution  $\theta^*$  after training a certain number of epochs with stochastic gradient descend. By the assumption on the conditional mean of the noisy gradient function and the assumption on  $S$ , the conditional covariance matrix is finite as well, i.e.,  $C = \lim_{t \rightarrow \infty} \mathbb{E}[\epsilon_{it} \epsilon_{it}^T | \epsilon_{i0}, \dots, \epsilon_{it-1}] < \infty$ ; hence, we can invoke the following result due to Polyak et al. (Polyak and Juditsky 1992):

$$\sqrt{t}(\bar{\theta}_t - \theta^*) \xrightarrow{\mathcal{D}} \mathcal{N}\left(0, \mathbf{H}(L(\theta^*))^{-1} C \mathbf{H}^T(L(\theta^*))^{-1}\right), \quad (11)$$

as  $t \rightarrow \infty$ . Here,  $\mathbf{H}$  is Hessian matrix,  $\theta^*$  is the global minimum of the loss function, and  $\bar{\theta}_t = \frac{1}{t} \sum_t \theta_t$ . Hence, for networks  $N_1$  and  $N_2$  and from Equation (11),  $\sqrt{t}(\bar{\theta}_{1t} - \theta^*)$  and  $\sqrt{t}(\bar{\theta}_{2t} - \theta^*)$  are asymptotically normal random vectors:

$$\sqrt{t}(\bar{\theta}_{1t} - \theta^*) \xrightarrow{\mathcal{D}} \mathcal{N}(0, \Sigma_1), \quad (12)$$

$$\sqrt{t}(\bar{\theta}_{2t} - \theta^*) \xrightarrow{\mathcal{D}} \mathcal{N}(0, \Sigma_2), \quad (13)$$

where  $\Sigma_1 = \mathbf{H}(L(\theta^*))^{-1} C_1 \mathbf{H}^T(L(\theta^*))^{-1}$ , and  $\Sigma_2 = \mathbf{H}(L(\theta^*))^{-1} C_2 \mathbf{H}^T(L(\theta^*))^{-1}$ . The Fisher Information

$F(\theta)$  is a continuous and differentiable function of  $\theta$ . Since it is also a positive definite matrix,  $F(\theta)^{1/2}$  is well-defined. Hence, by applying the Delta method to Equation (12), we have:

$$\sqrt{t}(\bar{F}_{1t}^{1/2} - F^{*1/2}) \xrightarrow{\mathcal{D}} \mathcal{N}(0, \Sigma_1^*), \quad (14)$$

where  $\bar{F}_{1t} = F(\bar{\theta}_{1t})$ , and the covariance matrix  $\Sigma_1^*$  is given by  $\Sigma_1^* = \mathbf{J}_\theta(\text{vec}(F(\theta^*)^{1/2})) \Sigma_1 \mathbf{J}_\theta(\text{vec}(F(\theta^*)^{1/2}))^T$ .

Here,  $\text{vec}()$  is the vectorization operator,  $\theta^*$  is a  $n \times 1$  vector of the optimum parameters,  $F(\theta^*)$  is a  $n \times n$  Matrix evaluated at the minimum, and  $\mathbf{J}_\theta(F(\theta^*))$  is a  $n^2 \times n$  Jacobian matrix of the Fisher Information Matrix. Similarly, from Equation (13), we have:

$$\sqrt{t}(\bar{F}_{2t}^{1/2} - F^{*1/2}) \xrightarrow{\mathcal{D}} \mathcal{N}(0, \Sigma_2^*), \quad (15)$$

where  $\Sigma_2^* = \mathbf{J}_\theta(\text{vec}(F(\theta^*)^{1/2})) \Sigma_2 \mathbf{J}_\theta(\text{vec}(F(\theta^*)^{1/2}))^T$ .

As a result,  $(\bar{F}_{1t}^{1/2} - \bar{F}_{2t}^{1/2})$  is asymptotically a normal random vector:

$$(\bar{F}_{1t}^{1/2} - \bar{F}_{2t}^{1/2}) \xrightarrow{\mathcal{D}} \mathcal{N}\left(0, V_1\right). \quad (16)$$

where  $V_1 = \frac{1}{t}(\Sigma_1^* + \Sigma_2^*)$ . As  $t$  approaches infinity,  $\frac{1}{t}(\Sigma_1^* + \Sigma_2^*) \rightarrow 0$ . As a result,  $d_t = \frac{1}{\sqrt{2}} \left\| \bar{F}_{1t}^{1/2} - \bar{F}_{2t}^{1/2} \right\|_F \xrightarrow{\mathcal{D}} 0$ .  $\square$

**Theorem 2.** *Let  $X_A$  be the dataset for the task  $T_A$  with the objective function  $L_A$ , and  $X_B$  be the dataset for the task  $T_B$  with the objective function  $L_B$ . Assume  $X_A$  and  $X_B$  have the same distribution. Consider an  $\varepsilon$ -approximation network  $N$  trained using both datasets  $X_A^{(1)}$  and  $X_B^{(1)}$  respectively with the objective functions  $L_A$  and  $L_B$  to result weights  $\theta_{A_t}$  and  $\theta_{B_t}$  at time  $t$ . Under the same assumptions on the moment of gradient noise in SGD algorithm and the loss function stated in Theorem 1, the FTD from the task  $A$  to the task  $B$  computed from the Fisher Information matrices of the average of estimated weights up to the current time  $t$  converges to a constant as  $t \rightarrow \infty$ . That is,*

$$d_t = \frac{1}{\sqrt{2}} \left\| \bar{F}_{A_t}^{1/2} - \bar{F}_{B_t}^{1/2} \right\|_F \xrightarrow{\mathcal{D}} \frac{1}{\sqrt{2}} \left\| F_A^{*1/2} - F_B^{*1/2} \right\|_F, \quad (17)$$

where  $\bar{F}_{A_t}$  is given by  $\bar{F}_{A_t} = F(\bar{\theta}_{A_t})$  with  $\bar{\theta}_{A_t} = \frac{1}{t} \sum_t \theta_{A_t}$ , and  $\bar{F}_{B_t}$  is defined in a similar way.

**Proof of Theorem 2.** Let  $\theta_{A_t}$  and  $\theta_{B_t}$  be the sets of weights at time  $t$  from the  $\varepsilon$ -approximation network  $N$  trained using both data sets  $X_A^{(1)}$  and  $X_B^{(1)}$ , respectively with the objective functions  $L_A$  and  $L_B$ . Since the objective functions are strongly convex, both of these sets of weights will obtain the optimum solutions  $\theta_A^*$  and  $\theta_B^*$  after training a certain number of epochs with stochastic gradient descend. Similar to the proof of Theorem 1, by invoking the Polyak et al. (Polyak and Juditsky 1992), random vectors of  $\sqrt{t}(\bar{\theta}_{A_t} - \theta_A^*)$  and  $\sqrt{t}(\bar{\theta}_{B_t} - \theta_B^*)$  are asymptotically normal:

$$\sqrt{t}(\bar{\theta}_{A_t} - \theta_A^*) \xrightarrow{\mathcal{D}} \mathcal{N}(0, \Sigma_A), \quad (18)$$

$$\sqrt{t}(\bar{\theta}_{B_t} - \theta_B^*) \xrightarrow{\mathcal{D}} \mathcal{N}(0, \Sigma_B), \quad (19)$$

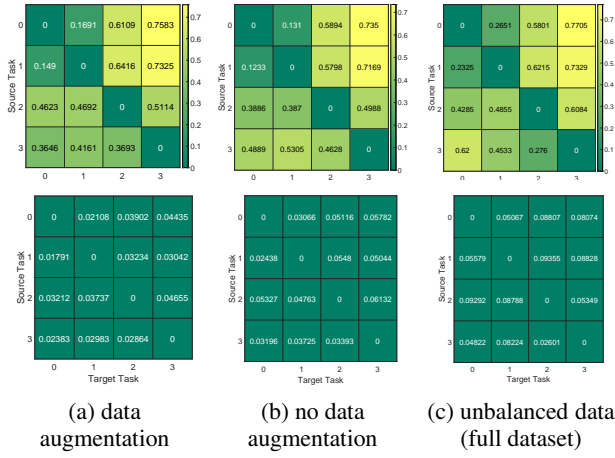


Figure 7: The effect of different initial settings on computing distance between tasks defined on CIFAR-10 using VGG-16 as the  $\varepsilon$ -approximation network. The top row shows the mean values and the bottom row denotes the standard deviation of distances over 10 different trials.

where  $\Sigma_A = \mathbf{H}(L(\theta_A^*))^{-1} C_A \mathbf{H}^T (L(\theta_A^*))^{-1}$ , and  $\Sigma_B = \mathbf{H}(L(\theta_B^*))^{-1} C_B \mathbf{H}^T (L(\theta_B^*))^{-1}$  (here,  $C_A$  and  $C_B$  denote the conditional covariance matrices, corresponding to the gradient noise in  $\theta_A^*$  and  $\theta_B^*$ , respectively). The Fisher Information  $F(\theta)$  is a continuous and differentiable function of  $\theta$ , and it is also a positive definite matrix; thus,  $F(\theta)^{1/2}$  is well-defined. Now, by applying the Delta method to Equation (18), we have:

$$(\bar{F}_{A_t}^{1/2} - F_A^{*1/2}) \xrightarrow{\mathcal{D}} \mathcal{N}(0, \frac{1}{t} \Sigma_A^*), \quad (20)$$

where  $\bar{F}_{A_t} = F(\bar{\theta}_{A_t})$ , and the covariance matrix is given by  $\Sigma_A^* = \mathbf{J}_\theta(\text{vec}(F(\theta_A^*)^{1/2})) \Sigma_A \mathbf{J}_\theta(\text{vec}(F(\theta_A^*)^{1/2}))^T$ . Likewise, from Equation (19), we have:

$$(\bar{F}_{B_t}^{1/2} - F_B^{*1/2}) \xrightarrow{\mathcal{D}} \mathcal{N}(0, \frac{1}{t} \Sigma_B^*), \quad (21)$$

where  $\bar{F}_{B_t} = F(\bar{\theta}_{B_t})$ , and the covariance matrix is given by  $\Sigma_B^* = \mathbf{J}_\theta(\text{vec}(F(\theta_B^*)^{1/2})) \mathbf{J}_\theta(\text{vec}(F(\theta_B^*)^{1/2}))^T$ . From Equation (20) and (21), we obtain:

$$(\bar{F}_{A_t}^{1/2} - \bar{F}_{B_t}^{1/2}) \xrightarrow{\mathcal{D}} \mathcal{N}(\mu_2, V_2), \quad (22)$$

where  $\mu_2 = (F_A^{*1/2} - F_B^{*1/2})$  and  $V_2 = \frac{1}{t}(\Sigma_A^* + \Sigma_B^*)$ . Since  $(\bar{F}_{A_t}^{1/2} - \bar{F}_{B_t}^{1/2}) - (F_A^{*1/2} - F_B^{*1/2})$  is asymptotically normal with the covariance goes to zero as  $t$  approaches infinity, all of the entries go to zero, we conclude that

$$d_t = \frac{1}{\sqrt{2}} \left\| \bar{F}_{A_t}^{1/2} - \bar{F}_{B_t}^{1/2} \right\|_F \xrightarrow{\mathcal{D}} \frac{1}{\sqrt{2}} \left\| F_A^{*1/2} - F_B^{*1/2} \right\|_F. \quad (23)$$

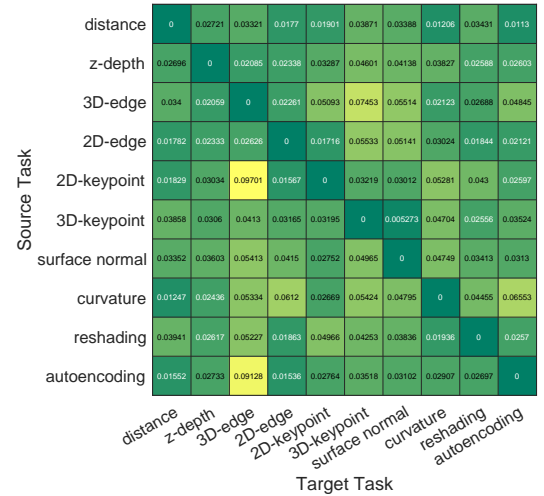
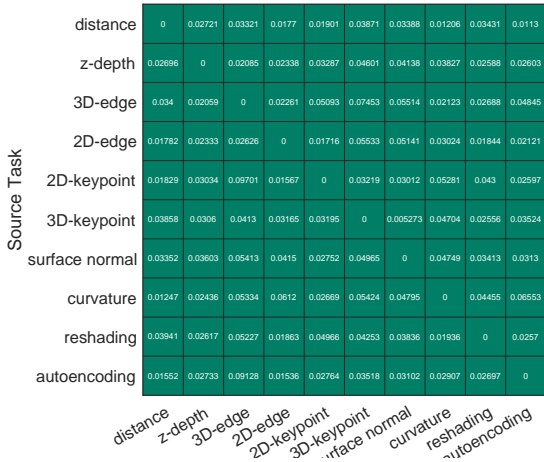
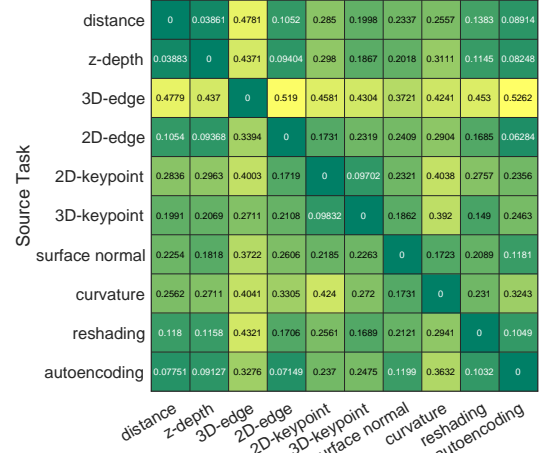


Figure 8: Distance from source tasks to the target tasks on Taskonomy dataset found by our approach and Taskonomy approach. The top panel shows the mean and the middle panel denotes the standard deviation values over 10 different trials. The bottom panel shows the task affinity found by brute-force approach (Zamir et al. 2018) after a single run.

This figure "graph.png" is available in "png" format from:

<http://arxiv.org/ps/2103.12827v3>

This figure "graph1.png" is available in "png" format from:

<http://arxiv.org/ps/2103.12827v3>